



ELSEVIER

Journal of Chromatography A, 952 (2002) 173–183

JOURNAL OF
CHROMATOGRAPHY A

www.elsevier.com/locate/chroma

Electron-capture detector and multiple negative ions of aromatic hydrocarbons

Edward S. Chen^{a,*}, Edward C.M. Chen^b

^aCenter for High Performance Software, Rice University, Houston, TX 77005, USA

^bUniversity of Houston Clear Lake, 4039 Drummond, Houston, TX 77025, USA

Received 31 October 2001; received in revised form 14 January 2002; accepted 14 January 2002

Abstract

Multiple electron affinities are identified in the temperature dependence of the electron-capture detector: naphthalene, 0.16, 0.13 ± 0.01 ; anthracene, 0.69, 0.60, 0.53 ± 0.01 ; tetracene 1.1, 0.88 ± 0.03 , 0.53 ± 0.05 ; pyrene, 0.61, 0.50 ± 0.02 ; azulene 0.90, 0.80, 0.70 ± 0.02 , 0.65, 0.55 ± 0.05 ; acenaphthylene, 0.80, 0.69, 0.60, 0.50 ± 0.05 ; and *c*-C₈H₈, 0.80, 0.70, 0.55 ± 0.02 ; (all in eV) These are obtained from a rigorous least squares procedure incorporating literature values and uncertainties. The adiabatic electron affinities for about 40 hydrocarbons listed in the US National Institute of Standards and Technology (NIST) tables are evaluated. The adiabatic electron affinity values not listed in NIST are biphenylene, 0.45 ± 0.05 eV and coronene, 0.8 ± 0.05 eV. Morse potential energy curves in the C–H dimensions illustrate multiple states for benzene and naphthalene. © 2002 Elsevier Science B.V. All rights reserved.

Keywords: Electron-capture detection; Detection, GC; Electron affinities; Polynuclear aromatic hydrocarbons; Hydrocarbons, aromatic

1. Introduction

It is now 40 years after the introduction of the electron-capture detector, ECD. It is an indispensable, simple, sensitive and selective detector for chromatography and the only device for the routine determination of thermodynamic and kinetic properties of thermal electron reactions at atmospheric pressure. One of these properties is the absolute energy of these reactions at absolute zero (0 K), the electron affinity, E_a . The adiabatic electron affinity, AE_a , is the difference between the ground state

energies of the anion and neutral, and is the largest value. Since the E_a are positive by convention, the AE_a is greater than zero because long range electron dipole or polarization attractions will be balanced by short range repulsions at some separation. This article is dedicated to Dr W.E. Wentworth, who is retiring from teaching and Dr James E. Lovelock, the inventor of the ECD who has recently written an autobiography. The kinetic model of the ECD was the result of the logical analysis of Wentworth and the data generated by the insatiable curiosity of Lovelock [1].

The E_a governs the response of the electron capture detector and the formation of negative ions in chemical ionization mass spectrometry [1–18]. For hydrocarbons it is important to fullerenes, com-

*Corresponding author.

E-mail addresses: echen@rice.edu (E.S. Chen), ecmc@hia.net (E.C.M. Chen).

bustion, electron conduction, nanoscale devices, environmental analysis, and the validation of theoretical calculations [19–21]. Before 1960, the E_a of aromatic hydrocarbons were obtained from half wave reduction potentials, $E_{1/2}$, or potentiometric titrations [5,8–11]. Since then, the ECD has been used to determine absolute E_a by measuring the equilibrium constant for thermal electron reactions at different temperatures [1–7]. In the 1990s, the E_a of aromatic hydrocarbons were measured with thermal charge transfer (TCT), photoelectron spectroscopy (PES), and kinetic dissociation experiments [12–18]. Only an approximate value of any measurand and its standard deviation, such as the E_a , can be obtained from a finite number experimental values, $y_i \pm u_i$. The “best” values are the properly weighted average and the random uncertainty, U_R . State assignments introduce systematic uncertainties, U_s , in any method. The demonstrated U_R are: PES and ECD, ± 0.01 eV; TCT and $E_{1/2}$, ± 0.02 – 0.05 eV depending on the reference E_a ; and kinetic dissociation, ± 0.1 eV.

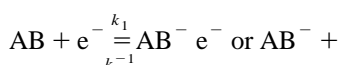
The US National Institute of Science and Technology (NIST) sequential list gives one value, the most recent: for example naphthalene, -0.19 and anthracene, 0.53 ± 0.005 eV. The average density functional calculated values are 0.05 and 0.8 eV, respectively. These deviate from the recent values by 0.2_5 eV, but agree with the AE_a ; $(0.16 - 0.05) + (0.69 - 0.8) = 0.0$ eV [18–21]. The NIST tables poses the question “Is the naphthalene radical anion bound or not?” By revisiting mass spectra, recognizing that multiple negative ion states exist, and obtaining the “best” adiabatic E_a for aromatic hydrocarbons, this question can be answered in the affirmative.

Multiple negative ion states have been observed in anion PES of cytosine, uracil, thymine, alone and with water and xenon [22,23]. Multiple anion states for O_2 and NO have been identified in ECD data [23–25]. The E_a , the partition function ratio or quotient, Q_{an} , for the anion and neutral, and $k_1 = A_1 T^{-1/2} \exp(-E_1/RT)$, the rate constant for thermal electron attachment, were obtained by incorporating literature values and their uncertainties in a sequential rigorous least squares procedure. Using this procedure the E_a are: naphthalene, $0.16, 0.13 \pm 0.01$; anthracene, $0.69, 0.60, 0.53 \pm 0.01$; tetracene $1.1, 0.88, \pm 0.03, 0.53 \pm 0.05$; pyrene, $0.60, 0.50 \pm 0.02$; azulene $0.90, 0.82, 0.72, \pm 0.02, 0.65, 0.55 \pm 0.05$;

acenaphthylene, $0.80, 0.69, 0.60, 0.50 \pm 0.05$; and $c\text{-C}_8\text{H}_8$, $0.80, 0.70, 0.55 \pm 0.05$ from ECD data. The AE_a from reduction potential data are: biphenylene, 0.45 ± 0.05 eV and coronene, 0.8 ± 0.1 eV [16,18,26]. The presentation of negative ion Morse potentials, and a simple method of obtaining E_a using ECD data are additional purposes of this paper [4,18,27].

2. Kinetic model of the electron-capture detector

The ECD data are: (I) original fixed frequency data for anthracene and acenaphthylene; (II) 1968 ethylene swarm data; (III) data for nitrobenzene and azulene obtained in 1980 using a ^{63}Ni detector; and (IV) constant current (cc) data published in 1981 [1–7]. The literature data and the PES for anthracene were digitized using the Unscant program [1–4,13–15,26]. In the ECD, electron current I_{e-} and I_b , with and without the test species (AB), and temperature, T , are recorded as a known amount of pure AB, elutes from the column. The ECD coefficient, is given by $K[AB] = \{I_b - I_{e-}\}/2I_e$, the Wentworth equation. For hydrocarbons, the reactions are:



$$K = \frac{k_N}{2(k_D)} \cdot \left[\frac{k_{1g}}{(k_{-1g} + k_N)} + \frac{k_{1x}}{(k_{-1x} + k_N)} \right] \quad (2)$$

$k_N = A_N$, $k_D = A_D$; $k_1 = A_1 T^{-1/2} \exp(-E_1/RT)$ and $k_{-1} = A_{-1} T \exp(-E_{-1}/RT)$, Q is the partition function ratio

$$KT^{3/2} = \frac{[L_R A_N]}{(2A_D)} \sum_{i=g,x} \frac{[(Q)_i \exp(E_{ai}/RT)]}{\left[1 + \frac{A_N T^{1/2} (Q)_i \exp(E_{ai}/RT)}{A_{i1} \exp(-E_{i1}/RT)} \right]} \quad (3)$$

The parameters are the E_a , Q , A_1 and E_1 . For each state, two limiting temperature regions are defined as: $\alpha(k_{-1} \gg k_N)$ and $\beta(k_N \gg k_{-1})$. In the higher temperature α region

$$\ln KT^{3/2} = \ln[L_R^*Q] + 12.43 + E_a/RT \quad (4)$$

L_R is a constant, and $\ln[h^3/(2\pi m_e k)^{3/2}] = 12.43$. The slope of the $\ln KT^{3/2}$ vs. $1/T$ is E_a/R . The E_1 and A_1 are determined in the lower temperature β region:

$$\ln KT^{1/2} = \ln(A_1/2A_D) - E_1/RT \quad (5)$$

The $A_{1(\max)}(E_1 = 0)$ is DeBA, the DeBroglie A_1 . The value of $\ln(\text{DeBA})$ is about 36.

The kinetic model of the ECD has been validated by its success in measuring fundamental physical properties, some of which have not been measured by any other technique. Of utmost importance is the equality of the many electron affinities measured by scaling the half wave reduction potentials and those obtained using the single state model. Additional support for the model is obtained by the verification of the rate constants for thermal electron attachment, detachment, and dissociation. These have been measured by other techniques, which include mass identification. The mass spectrometric identification of the ions in the ECD would be valuable but is not necessary. For example, the parent negative ions of naphthalene and anthracene were observed in the 1960s. In addition, the recent observation of anthracene and its hydrates is also discussed.

Possible side reactions with impurities in the carrier gas such as oxygen or water have been considered. They have been dismissed because of the exceedingly small concentration of the negative ions in the ECD. Thus, large concentrations of an impurity would have to be present to compete with attachment, detachment, or recombination. In addition, the cross sections for such reactions are much smaller than for the above reactions involving electrons. The only concerns that remain are the possibility of hyperthermal electrons and the identification of the states of the molecule. Furthermore, the values of the ECD parameters such as the Q_{an} , combined with the observed temperature dependence is such that there are no other plausible ions or reactions in the system.

Finally, the existence of multiple negative ion states have been verified by multiple independent techniques. This is perhaps the strongest evidence for the present analysis. The most important example is that of anthracene where PES data show multiple

states at exactly the same energies as that proposed in the ECD.

3. Results and discussion

In Table 1 are evaluated AE_a , excited state E_a and the NIST E_a . The ECD values, the photodetachment value for $c\text{-C}_8\text{H}_8$, the TCT values for benz[*a*]pyrene, perylene, tetracene and pentacene, the $E_{1/2}$ values for biphenylene and coronene, and the PES values for tetracene and perylene are the largest precise values and are the current “best” AE_a . The kinetic fragmentation values for anthracene, methyl anthracene, and pyrene are about the same, in agreement with the ECD data and are 0.65 ± 0.1 eV. This is assigned the average of the ECD values for pyrene and anthracene. All of the AE_a are supported by $E_{1/2}$ data and/or MINDO/3 calculations [5]. The effect of alkyl substitution can be determined from the AE_a of the alkyl benzenes and naphthalenes. The alkyl substitution increases the E_a by 0–0.04 eV. Each constant current determination is a determination of the AE_a for naphthalene which was used as an internal standard [3]. The kinetic fragmentation value for biphenylene is unexplainably high. Other kinetic fragmentation values and the reported PES values for anthracene, azulene, and coronene are assigned to excited states. These can be used to analyze the multiple states in the ECD as has been done for oxygen, NO, CS_2 , C_6F_6 anthracene and tetracene. The NIST entry for the $2\text{-C}_8\text{H}_7$ radical is erroneously listed as 4.85 eV, the C–H bond dissociation energy [18,27].

In Table 2 are the average values of the E_a , Q , A_1 and E_1 from the ECD data and the ethylene swarm values. The A_1 are approximately the DeBroglie A_1 . The Q values are generally close to one implying that the partition functions for the neutral and negative ions cancel except for the spin multiplicity. With Q , E_a and A_1 , only the E_1 value is required to calculate the temperature dependence for a given state. The E_1 are about zero for “maximum capture” compounds and increase as the response in the β region decreases.

In Figs. 1–5 plots of $\ln[KT^{3/2}]$ vs. $1000/T$ illustrate multiple states for azulene, acenaphthylene, anthracene, tetracene, O_2 and NO and the determi-

Table 1
Sequential list of evaluated hydrocarbon electron affinities determined with the ECD or $E_{1/2}$ methods (eV)

Molecule	AE_a	NIST	E_a^*	Methods
Benzene	0.01 ± 0.02	–	$-0.74, -1.12 \pm 0.05$	$E_{1/2}$, ET, no ECD
Benzene, 1,2,4,5-tetramethyl	0.07 ± 0.02	0.05		
Styrene	0.10 ± 0.05	–		
Benzene, 1,2,3,5-tetramethyl-	0.11 ± 0.02	0.11		
Benzene, hexamethyl-	0.12 ± 0.02	0.12		
Biphenyl	0.13 ± 0.02	0.13		
Naphthalene, 2-methyl-	0.14 ± 0.02	0.14		
Naphthalene, 1-methyl-	0.16 ± 0.02	0.16		
Naphthalene	0.16 ± 0.01	-0.20	$0.13 \pm 0.01, -0.15 \pm 0.05$	Ah-PES
Diphenylmethane	0.16 ± 0.02	0.16		
Naphthalene, 2,6-dimethyl-	0.16 ± 0.02	0.16		
Naphthalene, 2,3-dimethyl-	0.17 ± 0.02	0.17		
Indene	0.17 ± 0.02	0.17		
Benzene, pentamethyl-	0.18 ± 0.02	0.18		
Naphthalene, 2-ethyl-	0.19 ± 0.02	0.20		
Naphthalene, 1,4-dimethyl-	0.22 ± 0.02	0.25		
Fluorene	0.24 ± 0.02	0.28		
Triphenylene	0.29 ± 0.02	0.29		
Phenanthrene	0.30 ± 0.02	0.31		
Diphenylethyne	0.32 ± 0.02	0.32		
Ethylene, 1,1-diphenyl-	0.39 ± 0.02	0.39		
Stillbene	0.39 ± 0.02	0.39		
Biphenylene	0.45 ± 0.05	(0.89)		$E_{1/2}$, Kin, no ECD
Chrysene	0.42 ± 0.04	0.40		
Picene	0.50 ± 0.03	0.54		
Benz[<i>e</i>]pyrene	0.55 ± 0.03	0.53		
Benzo[<i>c</i>]phenanthrene	0.58 ± 0.01	0.55		
Pyrene	0.61 ± 0.02	0.50	$0.50 \pm 0.02, 0.65 \pm 0.1$	Kin
Anthracene, 1-methyl-	0.65 ± 0.02	0.55	0.65 ± 0.1	Kin
Dibenz[<i>a, j</i>]anthracene	0.67 ± 0.03	0.59		
Dibenz[<i>a, c</i>]anthracene	0.69 ± 0.03	–		
Anthracene	0.69 ± 0.01	0.53	$0.60 \pm 0.04, 0.53 \pm 0.01$	PES, TCT
Dibenz[<i>a, h</i>]anthracene	0.69 ± 0.03	0.59		
Benzo[<i>a</i>]anthracene	0.72 ± 0.01	0.39	0.4 ± 0.1	Kin
Benzo[<i>a</i>]pyrene	0.80 ± 0.03	0.82		
Coronene	0.80 ± 0.05	0.50	$0.5 \pm 0.1, 0.47 \pm 0.08$	$E_{1/2}$ Kin, PES no ECD
1,3,5,7- <i>c</i> -C ₈ H ₈	0.80 ± 0.05	0.55	$0.70 \pm 0.02, 0.57 \pm 0.02$	
Acenaphthylene	0.80 ± 0.02	0.40	$0.66, 0.60, 0.50 \pm 0.05$	
Fluoranthene	0.82 ± 0.04	0.63	0.66 ± 0.05	
Azulene	0.84 ± 0.05	0.69	$0.79, 0.68, 0.60$	
Benzo[<i>ghi</i>]perylene	0.89 ± 0.03	0.42	0.42 ± 0.1	$E_{1/2}$ Kin no ECD
Perylene	0.98 ± 0.01	0.97	0.35 ± 0.1	PES, TCT, Kin
Tetracene	1.10 ± 0.04	1.07	$0.88 \pm 0.04, 0.53 \pm 0.04$	
Pentacene	1.37 ± 0.05	1.39		TCT no ECD

nation of the highest, lowest and most precise values using the ECD: C₆F₅NO₂, 1.5 ± 0.05 , 1,2,4,5-(CH₃)₄C₆H₂, 0.07 ± 0.02 and acetophenone, 0.337 ± 0.002 eV. The latter have only an α region. The resolved states are shown by dotted lines. In Fig. 5 are ECD and anion PES data for O₂. In Fig. 6 are

negative ion mass spectra for benzene, naphthalene and anthracene. Fig. 7 gives anion PES data for anthracene and naphthalene hydrate. In Fig. 8 are Morse potential energy curves for the neutral and negative ions of benzene and naphthalene.

In Figs. 1 and 2 the constant current data are

Table 2
Experimental kinetic and thermodynamic properties of aromatic hydrocarbons

Compound	E_A (eV)	E_1 (eV)	$\ln A_1$	Q_{an}	Sources
Naphthalene	0.16 ± 0.02	0.21	34.2	1.0	See text
	0.13 ± 0.02	0.62	33.8	0.8	See text
Anthracene	0.69 ± 0.01	0.17	35.5	1	See text
	0.60 ± 0.02	0.11	35.5	0.9	See text
Pyrene	0.53 ± 0.01	0.18	35.8	1	See text
	0.61 ± 0.02	0.19	35.1	0.8	See text
c-C ₈ H ₈	0.50 ± 0.02	0.19	35.1	1	See text
	0.80 ± 0.05	0.3 ₆	36.8	1	This work
Acenaphthylene	0.70 ± 0.02	0.20	36.8	1	This work
	0.55 ± 0.02	0.10	34.6	0.1	See text
	0.82 ± 0.05	0.16	35.6	0.8	This work
	0.69 ± 0.02	0.13	35.6	0.8	This work
Azulene	0.60 ± 0.02	0.13	35.6	0.8	This work
	0.50 ± 0.05	0.06	35.6	0.8	This work
	0.90 ± 0.05	0.22	35.6	1	this work
	0.80 ± 0.02	0.13	35.6	1	This work
	0.70 ± 0.02	0.13	35.6	1	This work
Anthracene	0.65 ± 0.05	0.06	35.6	1	This work
	0.55 ± 0.05	0.03	35.6	1	This work
	0.69 ± 0.01	0.17	35.2	1	Ethylene swarm
	0.60 ± 0.02	0.1	35.2	0.9	Ethylene swarm
Pyrene	0.52 ± 0.01	0.14	35.2	1	Ethylene swarm
	0.61 ± 0.02	0.26	35.1	0.7	Ethylene swarm
Tetracene	0.50 ± 0.02	0.39	35.1	1	Ethylene swarm
	1.1 ± 0.04	0.95	37	1	Ethylene swarm
	0.88 ± 0.04	0.8	36	1×10^{-4}	Ethylene swarm
	0.53 ± 0.04	0.65	36	1	Ethylene swarm

compared with the constant frequency data for anthracene, azulene and acenaphthylene. The constant frequency data give the higher electron affinities because of the larger α region. The curves merge in the α region because the E_a and Q determine the slope. In the β region, the response depends on the A_D value and is larger the smaller the value of A_D . The constant current A_D is about 10^6 s⁻¹ while in the constant frequency mode, the A_D varies from 200 to 1000 s⁻¹ giving a much higher response in the β region and a larger region for determining the structure and the E_a values.

Five sets of azulene, four sets of naphthalene, four sets of anthracene and two sets of acenaphthylene data were analyzed. The constant current data better define the lower E_a . The similarity of the values for all states is apparent in Table 2. The lower E_a for pyrene is better defined by the larger temperature range of the ethylene swarm data. The ethylene swarm data originally gave an excited state E_a ,

tetracene, 0.88 eV and a Q value much lower than one [2,5]. The sequential two state model incorporated this value and the TCT value, 1.06 ± 0.04 eV. The original ethylene swarm value was obtained from the α region, 445 to 475 K and for many years was assigned to the AE_a . A lower temperature β region was identified but the high temperature negative slope was not explained. This is now attributed to E_{1g} , 0.95 eV.

3.1. Mass spectra and anion PES of oxygen, benzene, naphthalene and anthracene

The sequential list of positive values does not list naphthalene. Two values are found by looking up naphthalene, the ECD value, 0.15 ± 0.01 eV and -0.2 eV from the extrapolation of the peaks in anion hydrate PES, Ah-PES(n), to $n=0$. Depending on the extrapolation method, values of -0.2 , -0.09 , or -0.1 eV were reported. Another study reported $E_a =$

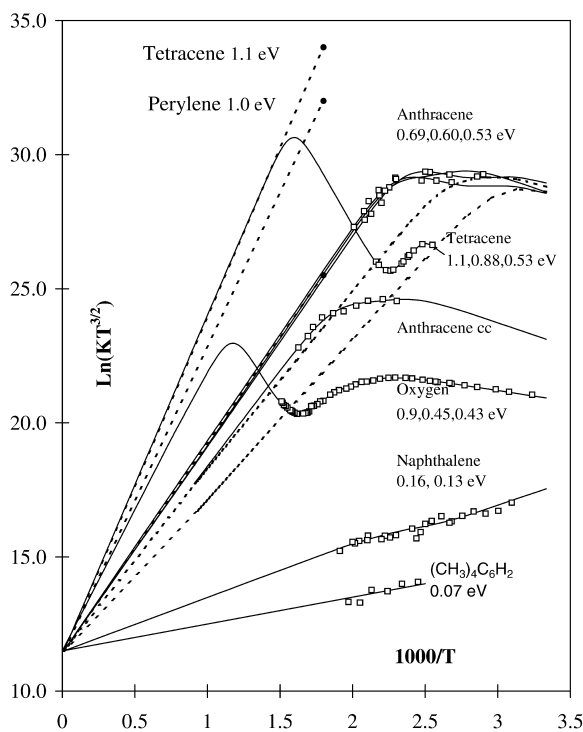


Fig. 1. Plot of molar response of the electron-capture detector as $\ln(KT^{3/2})$ vs. $1000/T$. O_2 , perylene and linear acenes.

-0.2 ± 0.05 eV = $0.13 - 0.28 - 0.05$ eV from the Ah-PES(1), the hydration energy and an empirical correction. This value was assigned to the AE_a because it agreed with an earlier value, the $M(-)$, 128, was not observed in the mass spectra, and only one negative ion state was considered.

A thorough literature search revealed that 128 had been observed by Von Ardenne et al. [28] in 1961 and Dougherty and Weisenberger [29] in a 1968 study of benzene, naphthalene and anthracene. Mass spectra from these studies are shown in Fig. 6 along with recent spectra for anthracene and naphthalene. The highest mass peak in the benzene spectrum is 79 or $[M+1]$. The M , $M+1$ and $M+2$ peaks for naphthalene and anthracene are apparent. The $M+1$ and $M+2$ ions could be $[M-1](-) \cdot H_2$ and $[M-2](-) \cdot 2H_2$. As seen in the 2000 scanned and digitized spectrum, peaks appear at 125, 126, 125+18, 130+18, $[128+n(18)]$, $n=1-4$ and $[32+n(18)]$ $n=$

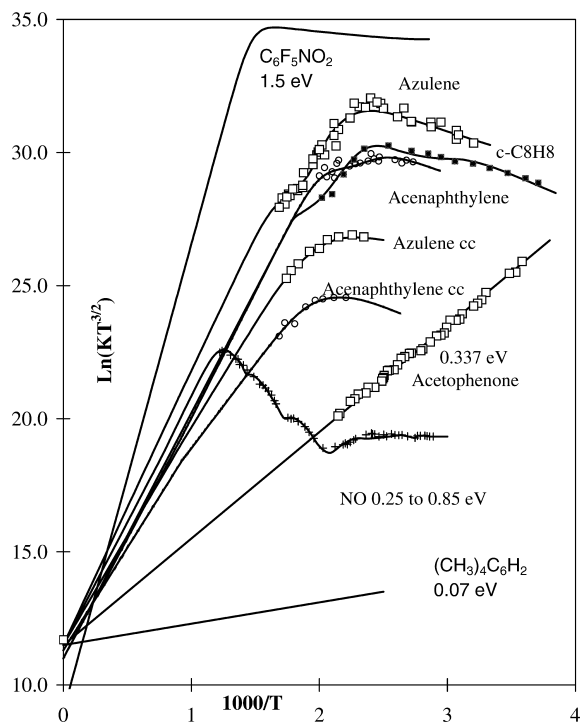


Fig. 2. Plot of molar response of the electron-capture detector as $\ln(KT^{3/2})$ vs. $1000/T$. Acetophenone, $C_6F_5NO_2$, azulene, acenaphthylene and NO. The dotted lines are the resolved peaks.

5–9. The parent ion is not observed, because of fragmentation, hydration and competitive reactions for electrons with O_2 .

The 1997 spectra of anthracene shows the anthracene $\cdot H_2O$ and a peak at m/z 32 for $O_2(-)$ but not its hydrates. The superoxide anion was formed by thermal charge transfer from anthracene, E_a , 0.69 ± 0.01 eV or its hydrate, E_a , 0.8 eV. This agrees with the E_a of 0.90 eV recently observed in the ECD data for O_2 , at 0.9 ± 0.05 eV, 0.74, 0.76 and 0.43, 0.45 ± 0.01 eV. The ECD data confirm the major peaks observed in the PES and spin-orbital coupling from Ref. [30], which begin at 0.43, 0.45 ± 0.01 eV in the PES shown in Fig. 5. There are small peaks at about 0.75, 0.95, and 1.07 eV corresponding to the states observed. In Fig. 7 are literature PES for anthracene and $C_{10}H_8(H_2O)$. The two peaks at 0.11 eV and 0.3 eV can be assigned to two states of the

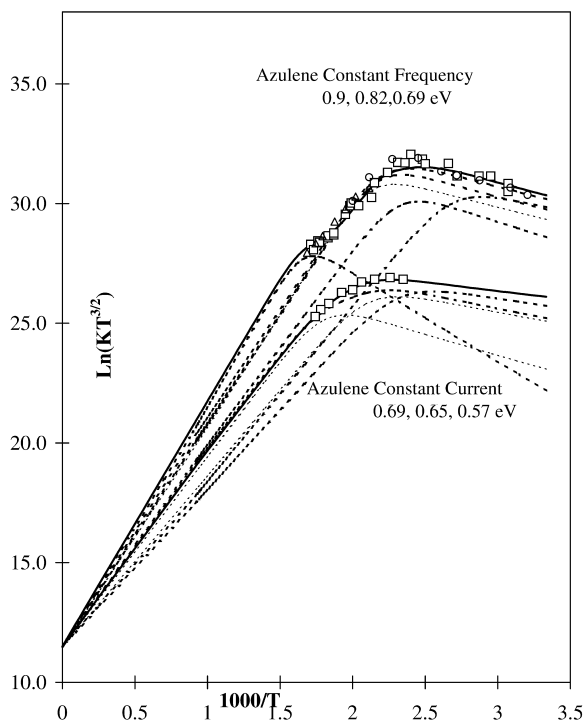


Fig. 3. Plot of molar response of the electron-capture detector as $\ln(KT^{3/2})$ vs. $1000/T$. The dotted lines are the resolved peaks.

anion of $C_{10}H_8(H_2O)$. With an hydration energy of 0.2 eV, the E_a of naphthalene are -0.1 and 0.1 ± 0.1 eV in agreement with the ECD and electron transmission values. The three E_a observed for anthracene in the ECD can be used to identify three origins at 0.53, 0.60, and 0.69 eV in the PES for anthracene. The different peak widths at 0.6 and 0.7 eV are apparent.

The AE_a of benzene is slightly larger than zero. The covalent E_a are associated with the dissociation limits, $R+H(-)$ and $R(-)+H$. These are separated by 0.35 eV, $E_a(\text{phenyl}) - E_a(H) = 1.1 - 0.75$ eV. The difference in the covalent E_a is $-0.74 - (-1.15$ eV) = 0.41 ± 0.05 eV. Consequently the two C–H bond dissociation energies in the anion are the same. Negative ion Morse potential energy curves for naphthalene can be calculated from the E_a , -0.20 , 0.13 , 0.16 eV leading to $R+H(-)$, $R1(-)+H$ and $R2(-)+H$. The neutral C–H bond dissociation energies are 4.85 eV, the E_a of the two naphthyl radicals

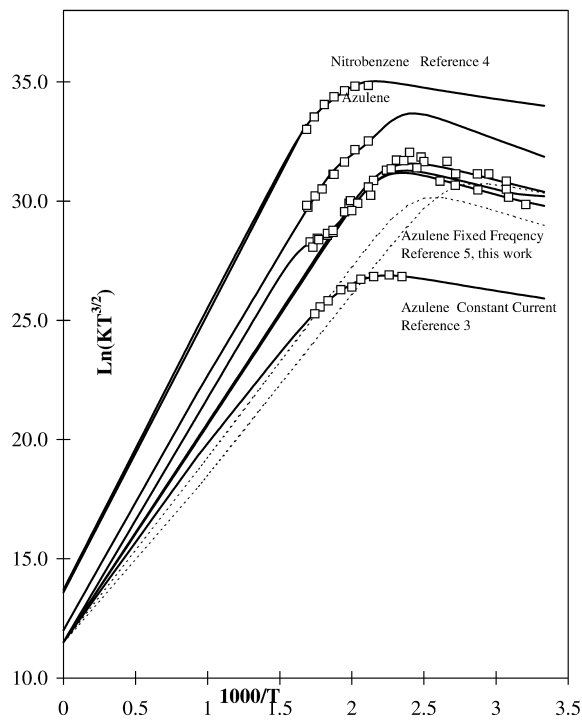


Fig. 4. Plot of molar response of the electron-capture detector as $\ln(KT^{3/2})$ vs. $1000/T$. Azulene and nitrobenzene. The dotted lines are the resolved peaks.

are 1.37 and 1.30 eV and the $E_a(H)$ is 0.75 eV so that these limits are experimentally determined [18,27]. Approximate curves for naphthalene and benzene are shown in shown in Fig. 8.

3.2. Azulene, $c\text{-}C_8H_8$, coronene and acenaphthylene

The E_a of azulene and $c\text{-}C_8H_8$, have been measured by ECD, PES, $E_{1/2}$ and TCT methods. That for coronene was determined by PES, kinetic fragmentation and $E_{1/2}$ and acenaphthylene by ECD and $E_{1/2}$ procedures. The AE_a for all of these have been verified using semi-empirical MINDO/3-CURES EC procedures. The ECD data for acenaphthylene are shown in Fig. 2. The constant frequency data and the constant current data can be fit with the same values of Q and A_1 . There is a systematic change in the

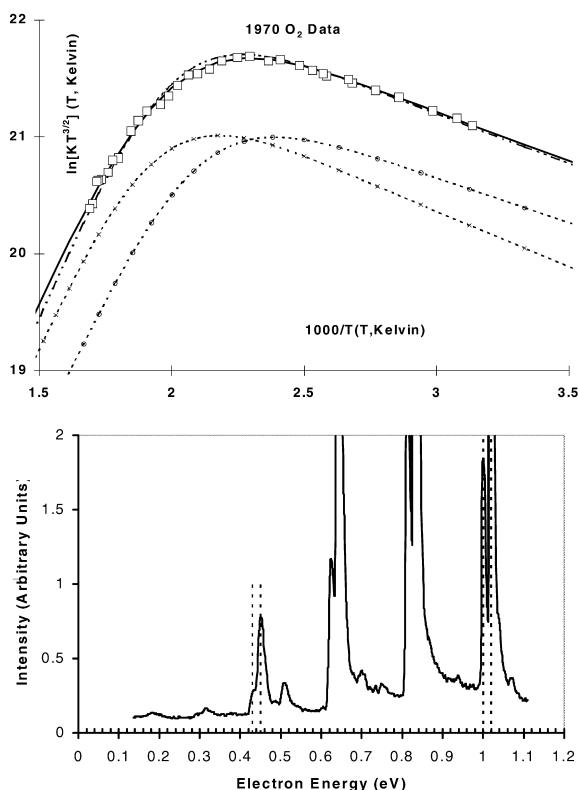


Fig. 5. Plot of molar response of the electron-capture detector as $\ln(KT^{3/2})$ vs. $1000/T$. O₂ with spin orbital coupling resolved peaks determined from literature data. Anion photoelectron spectra for O₂ from Ref. [30].

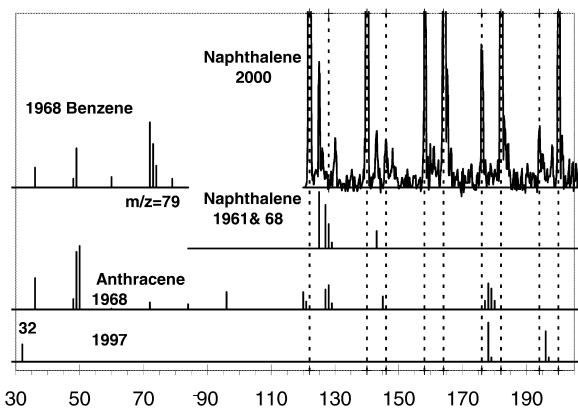


Fig. 6. Mass spectra for anthracene, naphthalene and benzene from Refs. [13,14,28,29]. The parent negative ions of naphthalene and anthracene are observed. The observation of O₂(⁻) in the presence of the anthracenehydrates(⁻) indicates that the electron affinity of O₂ is greater than 0.8 ± 0.05 eV.

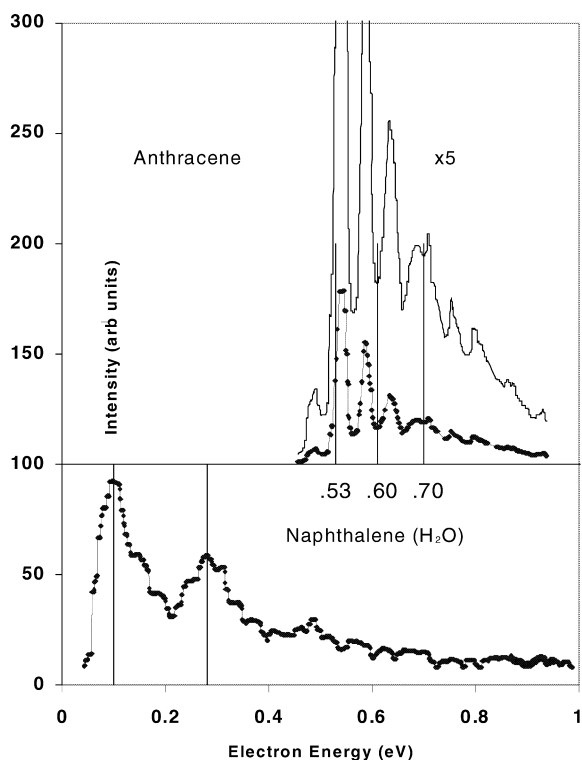


Fig. 7. Anion photoelectron spectra for anthracene and naphthalene H₂O from Refs. [13,14].

values of E_1 as shown in Table 2. Thus only one data point for each state is required to establish each of the four E_a . The highest value is supported by the $E_{1/2}$ measurements. Clearly there are also four types of acidic hydrogen atoms.

The E_a for $c\text{-C}_8\text{H}_8$ was reported as 0.58 ± 0.02 eV from the single state ECD model. However, the highest temperature data point indicates a higher energy state. The photodetachment value is less than 0.82 eV. There is no photoelectron spectroscopy value for cyclooctatetrene because the lowest energy peak at 1.1 eV corresponds to the vertical transition from the planar anion to the planar neutral. By estimating the energy to form the planar neutral as 0.45 eV, an estimated E_a of 0.65 eV was obtained. Thermal charge transfer and kinetic fragmentation values are 0.55 ± 0.02 and 0.6 ± 0.1 eV, respectively. By using these values, and the ECD data, the parameters shown in Table 2 are obtained and used

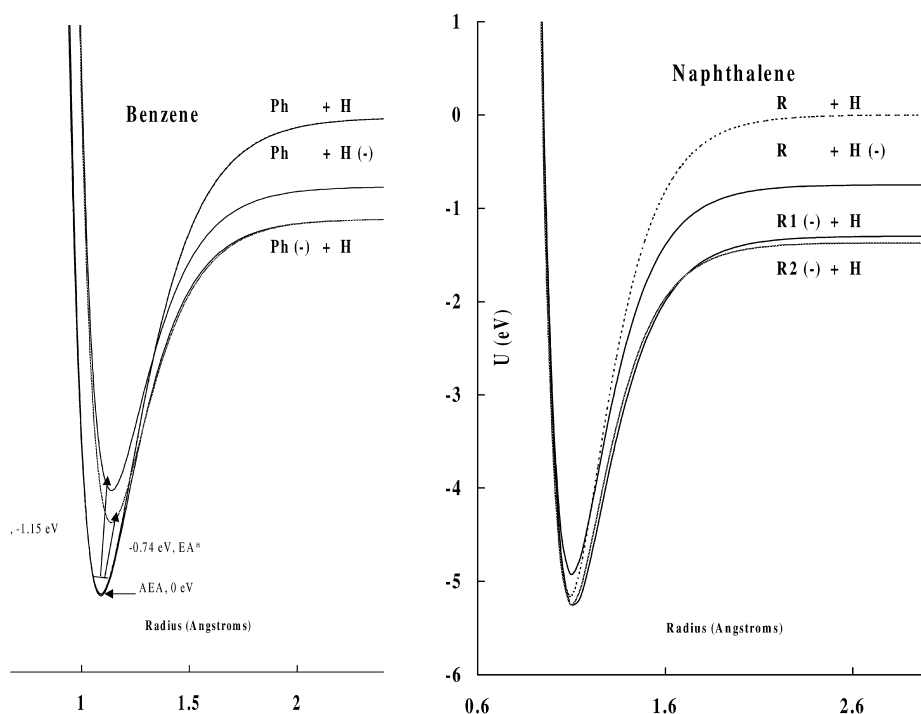


Fig. 8. Morse potential energy curves: Benzene and its negative ions; Naphthalene and its negative ions.

to calculate the ECD temperature dependence in Fig. 2.

The ECD data in Fig. 3 indicate five states for azulene, E_a , 0.55, 0.65, 0.70, 0.80 and 0.90 eV, one each for the different types of hydrogen atoms. The two lowest states are determined from the constant current data while the highest values are obtained from data in IV. In the PES data, not shown, only the highest three states are observed, 0.7, 0.8, and 0.9 eV. The data from Ref. [4] were obtained in 1980 and are a good example of the procedure for the independent determination of properties of electron molecule reactions. It also established that for nitrobenzene and azulene, the response is virtually independent of flow-rate at all temperatures investigated. For other compounds, there were some temperatures in which the response depends upon flow-rate and were hence dissociative. Because the AE_a of nitrobenzene has been determined by many different techniques as 1.00 ± 0.005 eV, the ECD response can be used to determine the instrumental parameters. In Fig. 5 is a plot of the data for these two compounds.

Although only a few temperature point are shown, there were multiple determinations as a function of flow-rate. By drawing a line from the highest temperature data point through the azulene data, a nominal E_a of 0.85 ± 0.05 eV is obtained. By using the two state model, two E_a are obtained, 0.90 ± 0.05 and 0.80 ± 0.02 eV in agreement with other constant frequency data as shown in Fig. 4.

3.3. Comparison of methods of determining electron affinities

The majority of molecular E_a have been determined by multiple procedures: ECD, TCT, PES, and $E_{1/2}$. In addition, the simple observation of a negative ion in the gas phase by mass spectrometry is an indication of a positive electron affinity. The reverse is however not true since the observation of a molecule with a low electron affinity depends on the lifetime of the ion relative to the time required to travel to the mass analyzer. The AE_a for O_2 , NO, NO_2 , SF_6 , CS_2 , about 100 hydrocarbons, cytosine,

thymine, uracil, *p*-benzoquinone, $C_6H_5NO_2$, CH_3NO_2 and C_6F_6 have been determined within the random uncertainties by two or more of the above techniques. All of these are supported by semi-empirical MCCI calculations. The E_a of perylene, tetracene, and nitrobenzene measured by all four of the above techniques are the same within the random uncertainties. In addition, all of these ions have been observed by mass spectrometry. This clearly demonstrates that each of the methods is capable of determining electron affinities of molecules within a nominal uncertainty. However, lower E_a were reported for each of the gas phase techniques. In particular, the constant current ECD values for the electron affinities of azulene, anthracene, acenaphthylene, pyrene, and the fixed frequency values for tetracene and CS_2 ; the PES values for O_2 , NO, anthracene, coronene, adenine, cytosine, uracil, thymine, and naphthalene and the TCT values for CS_2 and C_6F_6 were low. If multiple excited states are assumed for each of these, then all of the values are both accurate and precise. It had previously been demonstrated that two states could be observed in the ECD and PES for CS_2 and in the ECD for C_6F_6 . In the present study, multiple states for naphthalene, anthracene, tetracene, azulene, cyclooctatetraene have been identified in the ECD thus resolving some of the uncertainties in the adiabatic electron affinities of these molecules. Any values which differ from the highest value by more than the random uncertainties of the respective methods are assigned to excited states, specifically, the reported PES values for anthracene, coronene, CH_3NO_2 , O_2 and NO, the TCT values for C_6F_6 , $c-C_8H_8$, and CS_2 , and the kinetic fragmentation values for benzanthracene, coronene, perylene, and benzoperylene are excited state values. The only value which can not be explained by an excited state is the high value for biphenylene.

4. Conclusions

The AE_a and excited state E_a for benzene, naphthalene, anthracene, tetracene, azulene, cyclooctatetraene, and other hydrocarbons have been identified in data from the ECD. These are obtained from a rigorous least squares analysis of the two state model

incorporating literature values and uncertainties. The adiabatic electron affinities for about 40 hydrocarbons listed in the NIST tables are evaluated including biphenylene, 0.45 eV and coronene, 0.8 eV. Morse potential energy curves in the C–H dimension illustrate three states for benzene and naphthalene. The substitution of a methyl group for hydrogen in benzene and naphthalene has little effect on the E_a or slightly increases the value. The values for anthracene, methylantracene, and pyrene from kinetic fragmentation experiments are the same, 0.65 ± 0.1 eV, and agree with the ECD data. The negative ion states for hydrocarbons are related to the gas phase acidities as illustrated by Morse potential energy curves. The electron capture detector is a valuable tool for determining kinetic and thermodynamic data for thermal electron reactions. It can be used to routinely determine the absolute E_a , the partition function ratio for the equilibrium constant and the rate constant for thermal electron attachment and detachment at atmospheric pressure for small amounts of chromatographically purified samples. By adjusting operating conditions in the constant current mode, different electronic states can be probed. Other potentially interesting variable which can be adjusted in the ECD to study ion molecule reactions are pressure, and dopant gas and the flow-rate to determine the mechanism.

References

- [1] W.E. Wentworth, E.C.M. Chen, J.E. Lovelock, J. Phys. Chem. 70 (1966) 445.
- [2] L.E. Lyons, G.C. Morris, L.J. Warren, J. Phys. Chem. 72 (1968) 3677.
- [3] L. Wojnarovits, G. Foldiak, J. Chromatogr. 206 (1981) 511.
- [4] M. Takeuchi, Bull. Chem. Soc. Jpn. 53 (1980) 2829.
- [5] E.C.M. Chen, W.E. Wentworth, Mol. Cryst. Liq. Cryst. 171 (1989) 271.
- [6] E.C.M. Chen, E.S. Chen, M.S. Milligan, W.E. Wentworth, J.R. Wiley, J. Phys. Chem. 96 (1992) 2385.
- [7] E.C.M. Chen, W.E. Wentworth, S. Carr, E.S. Chen, J. Chromatogr. A 827 (1998) 91.
- [8] E.S. Chen, E.C.M. Chen, N. Sane, L. Talley, N. Kozanecki, S. Shultze, J. Chem. Phys. 110 (1999) 9321.
- [9] E.S. Chen, E.C.M. Chen, N. Sane, S. Shultze, Bioelectrochem. Bioenerget. 48 (1999) 69.
- [10] G. Briegleb, Angew. Chem., Int. Ed. Engl. 3 (1964) 617.
- [11] M. Szwarc, Ions and Ion Pairs in Organic Reactions, Vol. 1, Wiley, New York, 1972.

- [12] L. Crocker, T.B. Wang, P. Kebarle, *J. Am. Chem. Soc.* 115 (1993) 7818.
- [13] J. Scheidt, R. Weinkauff, *Chem. Phys. Lett.* 266 (1997) 201.
- [14] S.A. Lyapustina, S. Xu, J.M. Niles, K.H. Bowen, *J. Chem. Phys.* 112 (2000) 6643.
- [15] J. Schiedt, J. Knott, K. Le Barbu, E.W. Schlag, R. Weinkauff, *J. Chem. Phys.* 113 (2000) 9470.
- [16] G.D. Chen, R.G. Cooks, *J. Mass Spectrom.* 30 (1995) 1167.
- [17] K.M. Erwin, *Chem. Rev.* 101 (2001) 3001.
- [18] National Institute of Standards and Technology Chemistry WebBook [<http://webbook.nist.gov/>], 2001.
- [19] C.E.H. Dessent, *Chem. Phys. Lett.* 330 (2000) 180.
- [20] A. Klimkans, S. Larsson, *Chem. Phys.* 189 (1994) 25.
- [21] J.C. Reinskirakafe, C.J. Barden, S.C. Brown, H.F. Schafer, *J. Phys. Chem. A* 105 (2001) 524.
- [22] J. Schiedt, R. Weinkauff, D.M. Neumark, E.W. Schlag, *Chem. Phys.* 239 (1998) 511.
- [23] E.C.M. Chen, E.S. Chen, *J. Phys. Chem. B* 104 (2000) 7835.
- [24] E.C.M. Chen, E.S. Chen, *J. Mol. Spectrosc.* (2001) in press.
- [25] E.C.M. Chen, E.S. Chen, *Phys. Rev. A* (2001) in press.
- [26] M.A. Duncan, A.M. Knight, Y. Negishi, S. Nagao, Y. Nakamura, A. Kato, A. Nakajima, K. Kaya, *Chem. Phys. Lett.* 309 (1999) 49.
- [27] D.R. Reed, S.R. Kass, *J. Mass Spectrom.* 35 (2000) 534.
- [28] M. Von Ardenne, K. Steinfelder, R. Tummler, *Angew. Chem.* 73 (1961) 135.
- [29] R.C. Dougherty, C.R. Weisenberger, *J. Am. Chem. Soc.* 90 (1968) 6570.
- [30] J. Scheidt, R. Weinkauff, *Z. Naturforsch. A* 50 (1995) 1041.